# Localized Delivery of CRISPR/dCas9 via Layer-by-Layer Self-Assembling Peptide Coating on Nanofibers for Neural Tissue Engineering

Kunyu Zhang [a, 1], Wai Hon Chooi [a, 1], Shuang Liu [b], Jiah Shin Chin [a, c], Aoife Murray [d], Dean Nizetic [d, e], Du Cheng [b], Sing Yian Chew [a, d, *]

[a] School of Chemical & Biomedical Engineering, Nanyang Technological University, 637459 Singapore

[b] Key Laboratory for Polymeric Composite and Functional Materials of Ministry of Education, School of Materials Science and Engineering, Sun Yat-Sen University, Guangzhou 510275, China

[c] NTU Institute of Health Technologies, Interdisciplinary Graduate School, Nanyang Technological University, Singapore 639798, Singapore

[d] Lee Kong Chian School of Medicine, Nanyang Technological University, 308232 Singapore

[e] The Blizard Institute, Barts & The London School of Medicine, Queen Mary University of London, 4 Newark St., London E1 2AT, United Kingdom

[1] These authors contributed equally to this work.

* Corresponding author: sychew@ntu.edu.sg (S. Y. Chew)

**Keywords:** genome editing, gene delivery, CRISPR/Cas9, electrospinning, nerve regeneration

**Abstract:** The clustered regularly interspaced short palindromic repeat (CRISPR) systems have a wide variety of applications besides precise genome editing. In particular, the CRISPR/dCas9 system can be used to control specific gene expression by CRISPR activation (CRISPRa) or interference (CRISPRi). However, the safety concerns associated with viral vectors and the possible off-target issues of systemic administration remain huge concerns to be safe delivery methods for CRISPR/Cas9 systems. In this study, a layer-by-layer (LbL) self-assembling peptide (SAP) coating on nanofibers is developed to mediate localized delivery of CRISPR/dCas9 systems. Specifically, an amphiphilic negatively charged $SAP^-$ is first coated onto PCL nanofibers through strong hydrophobic interactions, and the pDNA complexes and positively charged $SAP^+$-RGD are then absorbed via electrostatic interactions. The SAP-coated scaffolds facilitate efficient loading and sustained release of the pDNA complexes, while enhancing cell adhesion and proliferation. As a proof of concept, the scaffolds are used to activate GDNF expression in mammalian cells, and the secreted GDNF subsequently promotes neurite outgrowth of rat neurons. These promising results suggest that the LbL self-assembling peptide coated nanofibers can be a new route to establish a bioactive interface, which provides a simple and efficient platform for the delivery of CRISPR/dCas9 systems for regenerative medicine.

## 1. Introduction

The clustered regularly interspaced short palindromic repeat (CRISPR) systems have evolved as powerful tools for precise genome editing in diverse biological applications [1, 2]. These systems use a single guide RNA (sgRNA) to direct the Cas9 nuclease to the target gene, resulting in gene deletion, insertion, and mutation [1-4]. Additionally, a transcriptional regulator can be fused to the dead Cas9 (dCas9), in which the two catalytic domains of Cas9 are inactivated and thus have no cleavage activity [5]. This allows the CRISPR/dCas9 system to be used to activate or interfere with specific gene expression, named CRISPR activation (CRISPRa) and CRISPR interference (CRISPRi) respectively [6, 7]. Unfortunately, apart from these promising features, challenges remained for the CRISPR/Cas9 system to be translated for clinical applications. Although viral vectors like adeno-associated virus (AAV) have shown great efficacy in CRISPR/Cas9 system delivery, the immunogenic response and long-term expression of viral vectors are still the main concerns [8, 9]. Meanwhile, the uptake of the vectors by undesired tissue or organ, especially during systemic administration, may cause off-target issues, which may lead to tumorigenic or other deleterious events. To overcome these limitations, we sought to develop an effective non-viral approach to deliver CRISPR/Cas9 components in a sustained and localized fashion, which is often required for tissue regeneration.

Polycaprolactone (PCL) is widely used for the fabrication of tissue engineering scaffolds by various techniques, including electrospinning and 3D printing [10, 11], owing to its machinability, structural stability, biocompatibility and biodegradability. However, the intrinsic hydrophobicity and absence of reactive ligands on PCL lead to ineffective cell adhesion and biomolecules immobilization, which hinders the further development of the scaffolds for tissue engineering. In addition, the chemical and biological stability of PCL makes it difficult for

surface modification. Lately, inspired by mussel adhesion chemistry, many groups, including ourselves, have demonstrated the easy-to-operate polydopamine coating strategy on PCL scaffolds, which could significantly enhance cell-substrate interactions and biomolecule immobilizations [12-19]. Such bioadhesive coating allowed effective scaffold-mediated delivery of Cas9-sgRNA ribonucleoprotein to cells [18]. However, although the mechanism is still unclear, the special surface chemistry of polydopamine has been reported to be not favorable to some sensitive cells [18]. Therefore, we aim to develop a novel coating strategy that is more cytocompatible and allows scaffold surface-mediated delivery of CRISPR/dCas9 system for CRISPRa. We delivered the systems through dCas9 plasmid DNA (pDNA) in this study due to its low cost, flexibility, and stability, which is useful for us to test on the new coating platform [20]. As a proof of concept, scaffold-mediated gene activation of Glial cell derived neurotrophic factor (GDNF) would be an interesting strategy to stimulate nerve regeneration as it delivers both topographical and biochemical cues to guide cellular and tissue regrowth.

In this study, we successfully fashioned a layer-by-layer (LbL) self-assembling peptide (SAP) coating on nanofibers that can mediate localized delivery of CRISPR/dCas9 system to promote neural regeneration. We first established an easy-to-operate approach for the bioactive functionalization of PCL nanofibers by SAP. These SAP-coated nanofibers exhibited good affinity towards pDNA/PEIpro complexes and hence could facilitate the efficient loading and sustained release of such complexes. Owing to the incorporation of RGD peptides, the scaffolds could also support cell adhesion and proliferation. Other than the RGD, our SAP-based scaffold design also allows facile incorporation of other bioactive peptides, thereby offering a superb platform for the investigation of cell-substrate interactions. Furthermore, due to these promising features, the scaffolds were capable of localized delivery of CRISPR/dCas9 system to activate

GDNF expression in mammalian cells, and the secreted GDNF could subsequently promote neurite outgrowth. We believe that the strategy reported in this work opens up a new route to establish a bioactive interface and a simple and efficient platform for the delivery of CRISPR/dCas9 systems for regenerative medicine.

## 2. Materials and methods

### *2.1. Materials*

Polycaprolactone (average Mw = 80000), 2,2,2-trifluoroethanol (TFE), heparin sodium salt and Triton-X 100 were purchased from Sigma-Aldrich (USA). Sodium hydroxide was purchased from Merck (Germany). All chemicals were used as received without further purification. The self-assembling peptide, $SAP^-$ (FEFEFEFE) and $SAP^+$-RGD (FKFKFKFKGGRGDSP), were synthesized by Genscript (USA) and characterized by HPLC and ESI-MS (Supplementary Methods Section 1. Characterization of SAP). Paraformaldehyde (PFA, 4%) was purchased from Santa Cruz Biotechnology. PEIpro transfection reagent was purchased from Polyplus (USA). Plasmid pSpCas9(BB)-2A-GFP (PX458) ("Cas9-GFP"; 9288 bp) was a gift from Feng Zhang (Addgene plasmid #48138) (Fig. S3) [21], and SP-dCas9-VPR ("dCas9-VPR"; 11,319 bp) was a gift from George Church (Addgene plasmid #63798) (Fig. S4) [22]. sgRNA expression vector (3028 bp) harboring a U6 promoter positioned upstream of the customized sgRNA sequence was obtained from Genscript (USA) and confirmed by DNA sequencing. The sequences of sgRNA are shown in Table S1. Fibroblast growth factor-2 was purchased from Peprotech (USA). M-MLV Reverse Transcriptase was obtained from Promega (USA). Human GDNF Duoset ELISA kit was purchased from R&D system (USA). Label IT nucleic acid labeling kit was obtained

from MirusBio (USA). SingleShot SYBR Green One-Step Kit and iTaq Universal SYBR Green One-Step Kit were purchased from Bio-Rad (USA). hMSCs were purchased from Lonza (Switzerland). All other cell culture reagents, Quant-iT PicoGreen dsDNA assay kit, Click-iT EdU cell proliferation assay kit and SYBR Select Master Mix were purchased from ThermoFisher (USA).

*2.2. Fabrication of LbL SAP-coated nanofibers*

Electrospun nanofibers were fabricated according to our previous report [18]. In brief, small strips of PCL films with thickness of 20 μm were adhered onto coverslips (Ø 18 mm) to create a 1 $cm^2$ area, and the coverslips were then placed on a rotation wheel (2400 rpm) for the collection of electrospun nanofibers. The PCL solution (14 wt% in TFE) was loaded into a syringe and dispensed at a fixed rate (1.0 mL $h^{-1}$) by a syringe pump. Voltages of +8 kV and −4 kV were then applied to the blunt needle tip and the rotating collector, respectively. The distance between spinneret and collector was set as 22 cm. The obtained electrospun fibers were sterilized by UV irradiation for 30 min followed by incubation in 70% ethanol for 10 min.

$SAP^-$ and $SAP^+$-RGD peptide powders were dissolved in sterilized 0.1 мм NaOH solution (1%, w/v) and 0.1 мм HCl (1%, w/v), respectively, and sonicated for 30 min prior to use. To get the LbL assembled scaffolds, 50 μL of $SAP^-$ solution (0.2%, w/v) was firstly dripped onto the PCL nanofibers to cover the 1 $cm^2$ scaffold area. After incubation at 37 °C for 2 h, the scaffolds were rinsed with DI $H_2O$ to remove uncombined peptides. 4 μL of PEIpro (1 mg/mL) were diluted in DI $H_2O$ before complexation with 4 μg of plasmids (N/P = 8). The complexation was performed

at room temperature for 15 min and then placed onto the scaffolds to allow adsorption at 37 °C for 1 h. The unbonded complexes were removed by washing with DI $H_2O$, and 50 μL of $SAP^+$-RGD solution (0.2%, w/v) was then added onto the scaffolds. After incubation at 37 °C for 2 h, the scaffolds were rinsed again with DI $H_2O$ to remove uncombined peptides. To investigate the sequential alternation of surface charges during LbL coating, the PCL nanoparticles (Ø ~ 400 nm) were coated with the same protocol and the zeta-potential was measured by Malvern Nano-ZS Zeta Sizer after each step. The experiment was repeated 3 times.

*2.3. SEM characterization of scaffolds*

The lyophilized samples were sputter-coated with platinum at 10 mA for 100 s, and then the surface morphology of the scaffolds was observed under a scanning electron microscope (SEM, JOEL, JSM-6390LA) at a 10-kV accelerating voltage. The average fiber diameters were measured by ImageJ (NIH) with at least 100 fibers per sample.

*2.4. Water contact angle measurements*

To study the surface wettability of SAP-coated PCL scaffolds, the static water contact angles of PCL, PCL@$SAP^-$ and PCL@$SAP^-$@$SAP^+$-RGD scaffolds were measured by the sessile drop method using a contact angle analyzer (Kruss DSA 25). The droplet volume was set as 2 μL. Measurements were carried out at least 3 times for each scaffold.

*2.5. FT-IR measurements*

To evaluate changes in chemical bond characteristics of the PCL scaffolds before and after SAP coating, FTIR was carried out by using a Fourier-transform infrared spectrometer (PerkinElmer Spectrum One). Spectra were acquired in the 400 – 4000 $cm^{-1}$. The samples were subjected to flash freezing and lyophilization prior to the measurement.

*2.6. Characterizations of complex loading and release*

To visualize the distribution of pDNA/PEIpro complexes on the scaffolds, pDNA was tagged with MFP488 using Label IT nucleic acid labeling kit as per the manufacturer's instructions. The MFP488-tagged pDNA was then complexed with PEIpro and adsorbed onto the scaffolds according to the protocol mentioned above. The scaffolds were then visualized under an epifluorescence microscope (Leica DMi8).

To test the loading efficiency of the pDNA/PEIpro complexes on the scaffolds, the rinsate during coating processes was collected carefully. After de-complexion from the pDNA/PEIpro complexes using heparin sodium salt (1:1 v/v, 20 μg $mL^{-1}$), the amount of pDNA in the rinsate was determined using the Quant-iT PicoGreen dsDNA assay kit according to manufacturer's protocol. The experimental loading efficiencies were computed using the following equation:

$$\text{Loading efficiency (\%)} = \frac{m_t - m_u - m_l}{m_t} \times 100\%$$

where $m_t$ is the total mass of pDNA used for loading, $m_u$ is the mass of unbound pDNA (pDNA remained in the complex coating solution) and $m_l$ the mass of pDNA loss during the coating of $SAP^+$-RGD (pDNA released into the $SAP^+$-RGD coating solution).

Subsequently, the scaffolds were incubated with 1 mL of PBS at 37 °C. While culture media better mimics the cell culture condition, the other components in the culture media or serum protein may affect the DNA assay reactions and plate reader readings. At each time point, 1 mL of PBS was collected from each sample and replaced with an equal volume of fresh PBS. The supernatant was then used to measure the amount of pDNA by the same protocol mentioned above.

*2.7. Cell culture*

U2OS cells were a generous gift from Professor Wenting Zhao at Nanyang Technological University. The U2OS cells and hMSCs were cultured in high-glucose DMEM with GlutaMAX, supplemented with 10% fetal bovine serum and 1% penicillin/streptomycin. The medium change was performed every 2-3 days. hNPCs were generated from induced-pluripotent stem cells as described previously [23]. The cells were cultured on poly-L-ornithine and laminin-coated culture dishes in maintenance medium, which consisted of DMEM/F12 supplemented with 1% glutaMAX, 1% N2 supplement, 2% B27 supplement, 1% penicillin/streptomycin and 20 ng $mL^{-1}$ FGF2. All the cells were cultured in a humidified incubator at 37 °C and 5% $CO_2$. Passage 6 hMSCs and passage 9 hNPCs were used in this study.

*2.8. Cell adhesion, proliferation and scaffold-mediated local transfection*

To assess the effects of different surface coatings on cell adhesion, U2OS and hMSCs were seeded at a density of 10,000 cells $cm^{-2}$, while hNPCs were seeded at a density of 50,000 cells $cm^{-2}$. To assess the effects of the SAP-coating on cell proliferation, the cell-seeded scaffolds were incubated with 10 mM EdU for 24 h before being fixed with 4% PFA. The scaffolds were permeabilized with 0.25% Triton-X then stained with the Click-iT reaction cocktail and Hoechst 33342. In each group, over 10 images from at least 3 scaffolds were taken at 20×, and at least 200 cells were quantified. The number of nuclei and EdU labelled nuclei were counted. For scaffold-mediated local transfection experiments, the Cas9-GFP plasmid was used, in which the 2A-GFP was fused to Cas9 to allow the detection of Cas9 expression in the transfected cells, and the U2OS cells were also seeded at a density of 10,000 cells $cm^{-2}$. After incubation at 37 °C for 48 h, the cells were fixed with 4% PFA solution for 10 min and then permeabilized in 0.25% Triton-X 100 in PBS for 15 min at room temperature. For morphology studies, the cytoskeleton was stained with Alexa Fluor 555 phalloidin or Alexa Fluor 488 phalloidin, and nuclei were stained with DAPI. Fluorescent images were acquired with an epifluorescence microscope (Leica DMi8) and analyzed using Image J (NIH). In each group, over 10 images from at least 3 scaffolds were taken using a 20× objective, and at least 50 cells were quantified. The circularity of cells was computed using the following equation:

$$C = 4\pi AP^{-2}$$

where A is the area occupied by cell and P is the perimeter of cell. Higher circularity means less spreading. In addition, the total cell number was counted by DAPI, while the $GFP^{+}$ cells were counted based on the co-localization of GFP and DAPI signals.

### *2.9. Subcutaneous implantation*

To assess the biocompatibility of the SAP-coated scaffolds *in vivo*, 1 × 1 cm PCL fiber scaffolds with thickness of 94 ± 4.7 μm were prepared with or without SAP coating according to the procedure mentioned. All experimental procedures that involved animals were performed in accordance with the Nanyang Technological University's Institutional Animal Care and Use Committee, (IACUC, NTU) guidelines. Sprague-Dawley rats (8 weeks, 200-250g) were anesthetized with isoflurane before shaving their backs. Thereafter, subcutaneous pockets were created using surgical scissors after 1.2 cm incisions were made beside the spinal column. Following that, the scaffolds were inserted into the subcutaneous pockets such that each animal received both plain and SAP-coated scaffolds. The wounds were then closed with suture and the animals were observed for 5 days. After 5 days, animals were sacrificed and the tissues enclosing scaffolds were harvested and fixed in 4% PFA overnight. Thereafter, the scaffolds were dehydrated, embedded in paraffin and sectioned to obtain 5 μm thick sections. The sections were then stained with Haematoxylin and Eosin (H&E) and imaged with ZEISS Axio Scan.Z1 using a 20× objective. The images were then analyzed by an experimenter blinded to experimental groups. Semi-quantitative evaluation was performed on the scaffold biocompatibility based on fibrotic tissue formation, presence of macrophages (rounded morphology) at the boundary of the scaffold, and fibroblasts (elongated morphology) infiltration into the scaffold; using a scoring system, +: minimal, ++: some, +++: moderate, ++++: significant (n = 4 rats). To further evaluate inflammatory response towards the scaffolds, the number of macrophages and neutrophils in the scaffolds were counted. A total of 18 evenly distributed ROIs (50 μm × 50 μm) were assessed for each sample (n = 4 rats).

*2.10. Bolus transfection experiments*

A preliminary test has been performed with different transfection reagents, including Lipofectamine 3k, L-PEI, PEIpro, and JetOPTIMUS (Fig. S14). PEIpro demonstrated one of the highest transfection efficiency and acceptable toxicity and hence was used for the subsequent experiments. For gene activation experiments, U2OS cells were seeded onto 24-well plates at a density of 20,000 cells per well. Twenty-four hours after plating, cells were transfected with Cas9-GFP plasmids or a 1:1 mass ratio of dCas9 plasmid:sgRNA plasmids. A total plasmid mass of 0.5 μg per well was transfected using 0.5 μL per well of PEIpro reagent. For synergy experiments, the amount of total sgRNA was kept constant and the mass ratio of each sgRNA was 1:1 or 1:1:1. The cells were harvested 2 d after transfection, and gene expression analysis was performed.

*2.11. Scaffold-mediated gene activation in mammalian cells*

For exogenous gene-activation experiments, the dCas9 expression plasmids and sgRNA plasmids were co-delivered with a mass ratio of 1:1, and the sub-mass ratio of each sgRNAs was 1:1:1. U2OS cells were seeded onto the scaffolds at a density of 10,000 cells $cm^{-2}$ in 200 μL culture medium. The medium was sufficient to cover the 1 $cm^2$ scaffold area. Three experiments were performed. Gene activation was verified by gene expression analysis (Section 2.12). The amount of GDNF secreted by the U2OS cells on the scaffolds was quantified by ELISA. Specifically, the 200 μl medium was collected every 24 h and replaced with 200 μL fresh

medium for 3 days, and the collected medium was then stored at -80 °C for subsequent assays (Section 2.13). To test the bioactivity of the secreted GDNF, medium was collected after 3 days of culture without medium replacement. Thereafter, the collected medium was added to the cortical neurons and DRG explant cultures as conditioned medium (Section 2.14).

### *2.12. Gene expression analysis*

After 2 days of culture, cells seeded on the 24-well plates were lysed by TRIzol reagent, and RNA was extracted according to the manufacturer's instructions. The RNA concentration was determined by the NsD-1000 spectrophotometer (NanoDrop Technologies), and 500 ng of RNA from each sample were reverse transcribed into cDNA using M-MLV Reverse Transcriptase. Real-time PCR was performed on the StepOnePlus system (Applied Biosystems) using SYBR Select Master Mix. The sequences of the primers are listed in Table S2 and GAPDH was used as the housekeeping gene. The primers were checked to have similar amplification efficiency. The PCR parameter was 10 min at 95 °C, followed by 15 s at 95 °C and 1 min at 60 °C for 40 cycles. The relative gene expression was calculated using the $\Delta\Delta C_T$ method, where the fold difference was calculated using the expression $2^{-\Delta\Delta C_T}$. For cells that were seeded on the scaffolds, the cells were lysed by SingleShot SYBR Green One-Step Kit and PCR was performed with iTaq Universal SYBR Green One-Step Kit according to the manufacturer's instructions.

### *2.13. ELISA assay*

The amount of secreted GDNF in the medium was quantified using the media obtained in Section 2.11. Specifically, after the scaffolds were functionalized with SAP coatings and plasmids, U2OS cells were seeded onto the scaffolds at a density of 10,000 cells $cm^{-2}$ in 200 µl medium. The medium was collected every 24 h and replaced with 200 µl fresh medium for three days. The collected medium was stored in -80 °C freezer until quantification and was measured by using a human GDNF ELISA kit following the manufacturer' s instructions without dilution. In brief, 96-well microplate was coated with 100 µL/well of the Capture Antibody and incubated overnight at room temperature, followed by washing with wash buffer for three times. Thereafter, non-specific binding was blocked with Reagent Diluent at room temperature for 1 h prior to wash for three times. The samples and standards were then added into the coated wells (100 µL each) and incubated for 2 h at room temperature. The antigen was then incubated with 100 µL of Detection Antibody for 2 h, followed by the solution of Streptavidin-HRP A for 20 min in dark. The addition of Substrate Solution (100 µL each) started the color reaction which was stopped 20 min later with 50 µL of Stop Solution. The optical density of each well was immediately measured at 450 nm with a reference wavelength at 570 nm. GDNF concentrations were determined from the regression line for the GDNF standard ranging from 31.3 to 500 pg/mL. Each sample represents one scaffold. Medium from three control and CRISPRa-GDNF scaffolds was measured.

*2.14. Cortical neurons and DRG explants culture*

To test for the bioactivity of the GDNF secreted by the U2OS cells on the functionalized scaffolds, we transferred the conditioned medium to the neuron cultures and evaluated neurite

outgrowth. The conditioned media was obtained by collecting the 200 µl culture media from U2OS cells cultured on the control or CRISPRa-GDNF scaffolds for 3 days as mentioned in Section 2.11. Cortical neurons were isolated from P1 Sprague-Dawley rat pup brain cortices by trypsin digestion at 37 °C for 15 min. After the suspension was passed through a 70 µm cell strainer, the dissociated cortical neurons were seeded on aligned nanofiber scaffolds at 30,000 cells $cm^{-2}$ in the conditioned medium at 37 °C [24]. DRG explants were harvested from P3 rat pups and all the meninges from the DRGs were taken off. Two DRG explants were seeded onto each aligned nanofiber scaffolds with 1 $cm^2$ area. The cortical neurons and DRG explants were then cultured in the 200 µl of the collected conditioned medium (Section 2.11) at 37 °C. After cultured for 3 days, cortical neurons and DRG explants were fixed with 4% PFA at room temperature for 20 min. After washing in PBS for 3 times, cortical neurons and DRG explants were permeabilized with 0.3% Triton X-100 followed by blocking with 10% goat serum for 1 h at room temperature. Thereafter, the samples were incubated with mouse anti-βIII-Tubulin (Tuj-1, 1:1000 dilution) overnight at 4 °C, followed by incubation in goat anti-mouse Alexa Fluor 555 secondary antibody for 2 h at room temperature. Cell nuclei were counterstained with DAPI. Fluorescent images were acquired with an epifluorescence microscope (Leica DMi8) and analyzed using Image J (NIH). At least 5 scaffolds of each group were used in this experiment. For cortical neurons, 10 images were taken using a 20× objective for each scaffold and at least 90 cells were quantified for each group. For each DRG, the ten longest neurites were measured and averaged to determine the average neurite outgrowth length for each sample. At least 5 DRG explants were analyzed from each group.

### *2.15. Statistical analysis*

All values were presented as mean ± standard deviation (S.D). Outlier analysis was performed to exclude significant outliers from the subsequent analyses. One-way ANOVA and Tukey's post-hoc tests were used for samples that passed the homogeneity test. Otherwise, Kruskal–Wallis and Mann – Whitney U test were used for pairwise analysis. Student's t-test was used to compare 2 independent samples. Tests were conducted with a 95% confidence interval ($\alpha = 0.05$).

## 3. Results

### *3.1. Preparation and characterization of LbL coated PCL nanofibers*

The self-assembling peptides ($SAP^-$, $SAP^+$-RGD) were synthesized by Fmoc solid-phase method. High-pressure liquid chromatography (HPLC) confirmed that the purity of the peptides was 97.8% and 99.2%, respectively, and the mass spectrometry results assured the correct molecular weight of these peptides (Fig. S1, S2). The PCL nanofibers were fabricated using an electrospinning technique, and the LbL coating was then performed based on the strategy as illustrated in Scheme 1. $SAP^-$, the amphiphilic peptide bearing negative charges, was firstly coated onto the PCL scaffolds by dip-coating, resulting in the negative surface charge. Subsequently, the positively charged pDNA/PEIpro complexes and $SAP^+$-RGD were coated. This assembly process can also take place on the surface of PCL nanoparticles and was confirmed by the sequential alternation of zeta-potential (Fig. S5). The strong hydrophobic interactions between the aromatic side chains of the β-sheet $SAP^-$ and the PCL molecules allowed the adsorption of $SAP^-$ onto the hydrophobic PCL surface, while the established negatively charged surface further facilitated the adsorption of pDNA/PEIpro complexes and subsequently $SAP^+$-RGD through electrostatic interactions.

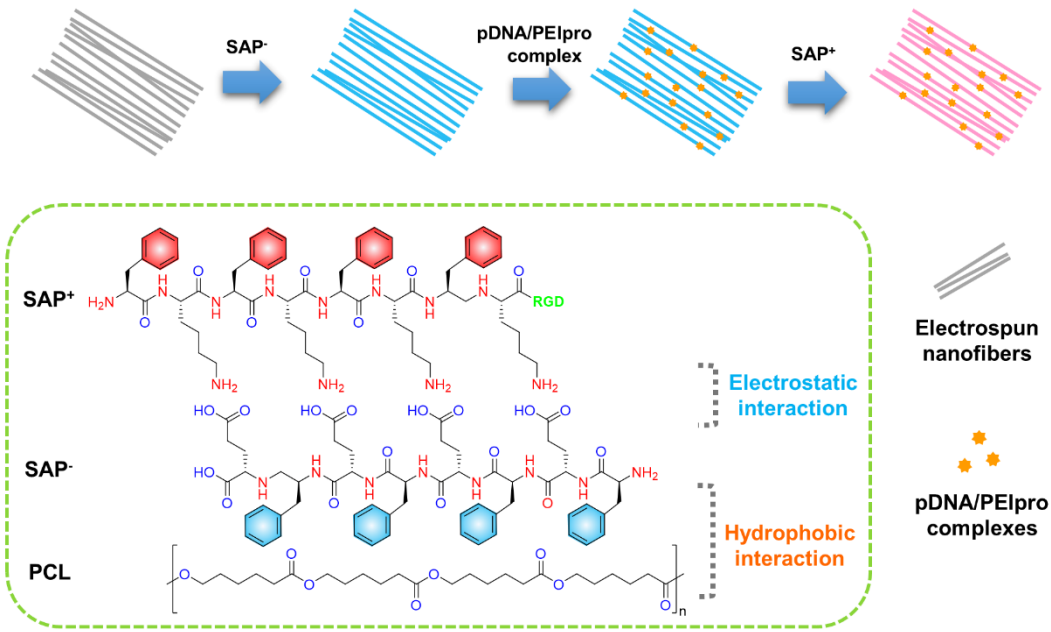


**Scheme 1. Schematic illustration of the layer-by-layer coating of SAPs on PCL nanofibers.**

As shown in the SEM images of the scaffolds (Fig. 1a), the SAP coatings did not mask the underlying fiber morphology. Specifically, the average fiber diameter of the plain PCL scaffolds was 929 ± 107 nm, while that of the $SAP^-$-coated scaffolds ("PCL@$SAP^-$") and $SAP^-/SAP^+$-RGD dual-coated scaffolds ("PCL@$SAP^-$@$SAP^+$-RGD") was 945 ± 103 nm and 958 ± 96 nm, respectively. This suggests that the SAP coatings did not significantly alter the topography of the aligned fibers.

Surface wettability is one of the most important surface properties that affect the cellular response towards an implanted substrate, including cell attachment, spreading, and proliferation. The contact angles of PCL and PCL@$SAP^-$ were 99.3 ± 3.0 ° and 35.3 ± 2.9 °, respectively. The significantly increased hydrophilicity suggests the successful coating of the negatively charged $SAP^-$. Subsequently, the adsorption of the positively charged PEI complexes and then the coating of $SAP^+$-RGD resulted in a slightly increased contact angle (52.3 ± 5.2 °). The contact angles of

the SAP-coated PCL scaffolds did not change significantly after incubation in phosphate-buffered saline (PBS) for at least 7 days (Fig. S6), indicating the good stability of SAP modification. Furthermore, we also characterized these scaffolds by comparing typical chemical bonds before and after SAP coating. Fourier transform infrared (FT-IR) spectroscopy measurements revealed plain PCL scaffolds exhibited the absorption peak at 1720 $cm^{-1}$, which is indicative of the -C=O stretching vibration of PCL (Fig. S7). After $SAP^-$ coating, two strong peaks at 3293 $cm^{-1}$ and 1635 $cm^{-1}$ were observed, and these were attributed to the -NH- stretching vibration and $-NH_2$ bending vibration of $SAP^-$, respectively. These findings collectively suggest that the SAP was successfully coated onto the PCL nanofibers.

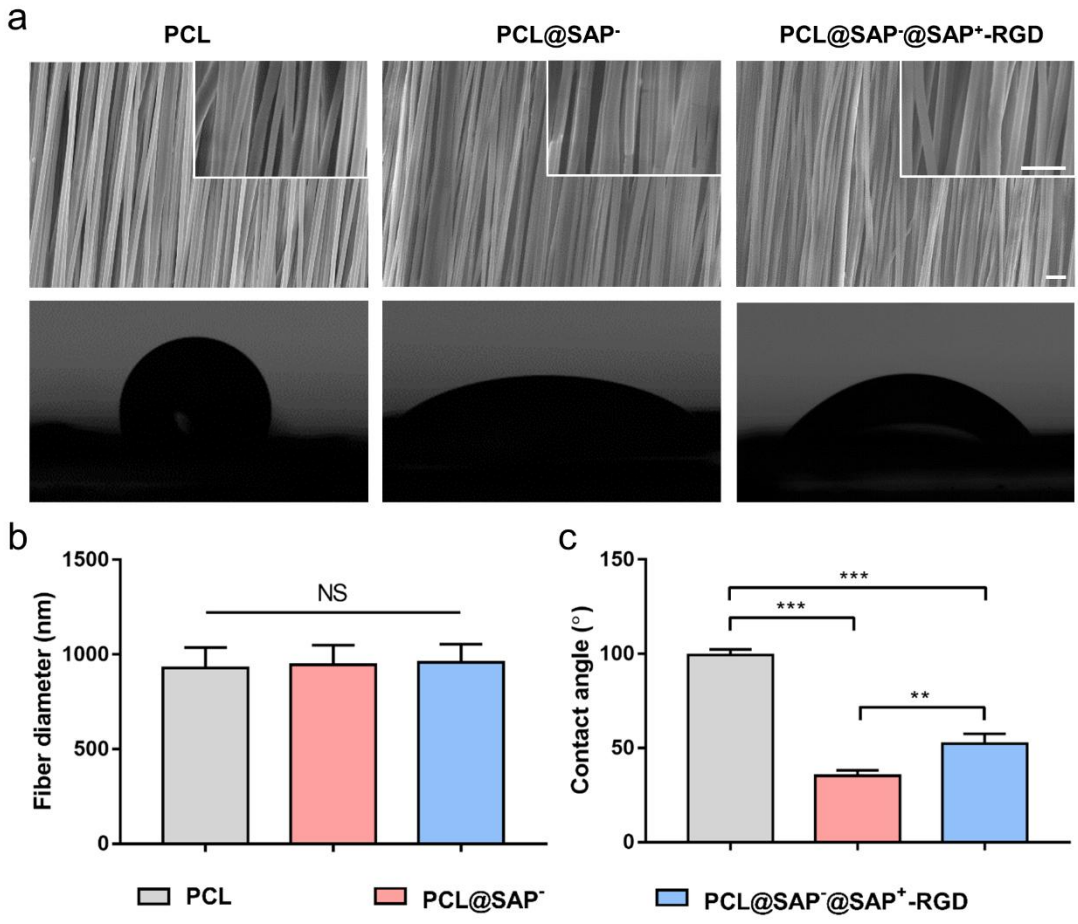

**Fig. 1. Characterization of SAP-coated scaffolds.** a) SEM images and photographs of water contact angles of the SAP-coated scaffolds; scale bar = 10 μm. b) Fiber diameters (n = 3) and c) water contact angles of the SAP-coated scaffolds (n =3); $^{***}p < 0.001$, "NS" indicates "no significance".

### *3.2. SAP-coated scaffolds mediated efficient loading and sustained release of pDNA/PEIpro complexes*

Polyethylenimine (PEI), a cationic polymer, is a widely used and cost-effective reagent for gene delivery. However, the N-propionyl groups in PEI molecules may reduce the number of protonatable nitrogen residues and hinder the nucleic acid condensation and endosomal escape. Therefore, the deacylated PEI, commercially known as PEIpro, was chosen for this work and shown to be superior for the mammalian cells [25]. As shown in Fig. S8, no significant difference was observed in the particle size and zeta potential of PEIpro/pDNA complexes with an increase in N/P ratio. Thus, the complexes of N/P = 8 with moderate positive charge (+8.4 ± 1.1 mV) and relatively small size (37.78 ± 11.06 nm) were chosen for all subsequent experiments. To visualize the distribution of the pDNA/PEIpro complexes on the scaffolds, fluorescently-tagged pDNA, MFP488-pDNA, was used. As shown in Fig. 2a, a uniform distribution of MFP488-pDNA/PEIpro complexes could be identified on the aligned fiber substrates. Specifically, the SAP-coated fibers, both PCL@SAP$^-$ and PCL@SAP$^-$@SAP$^+$-RGD, demonstrated significantly higher affinity to the complexes, and the loading efficiency of plain PCL, PCL@SAP$^-$, and PCL@SAP$^-$@SAP$^+$-RGD scaffolds was 82.9 ± 2.4%, 97.2 ± 2.6%, and 93.4 ± 3.7%, respectively (Fig. 2b). We next investigated the release kinetics of the complexes

from the scaffolds that were incubated in PBS at 37 °C (Fig. 2c). As compared to the plain PCL scaffolds in which the pDNA/PEIpro complexes were loosely entrapped, the SAP-coated scaffolds exhibited significantly smaller initial burst release and slower subsequent release of the complexes. These SAP-coated scaffolds were capable of releasing pDNA/PEIpro continuously for at least a week. Notably, the PCL@$SAP^-$@$SAP^+$-RGD scaffolds demonstrated similar loading efficiency and release rate as that of the PCL@$SAP^-$ scaffolds, indicating that the subsequent coating of $SAP^+$-RGD did not significantly affect the loading and release profile of the complexes. It is believed that the electrostatic interactions between the negatively charged $SAP^-$ and positively charged pDNA/PEIpro complexes may help to immobilize these complexes on the scaffolds and slow down the release. In contrast, the faster release of complexes from the plain PCL scaffolds may be due to the lack of such stabilizing mechanisms. Moreover, this platform constructed by electrostatic interactions is also capable of trapping other complexes, which include some of the commonly used RNA/Lipofectamine, protein/Lipofectamine, and pDNA/semiconducting polymer nanoparticles (SPNs) (Fig. S9). Hence, the platform is believed to be an effective approach for the delivery of various positively charged nano-complexes.

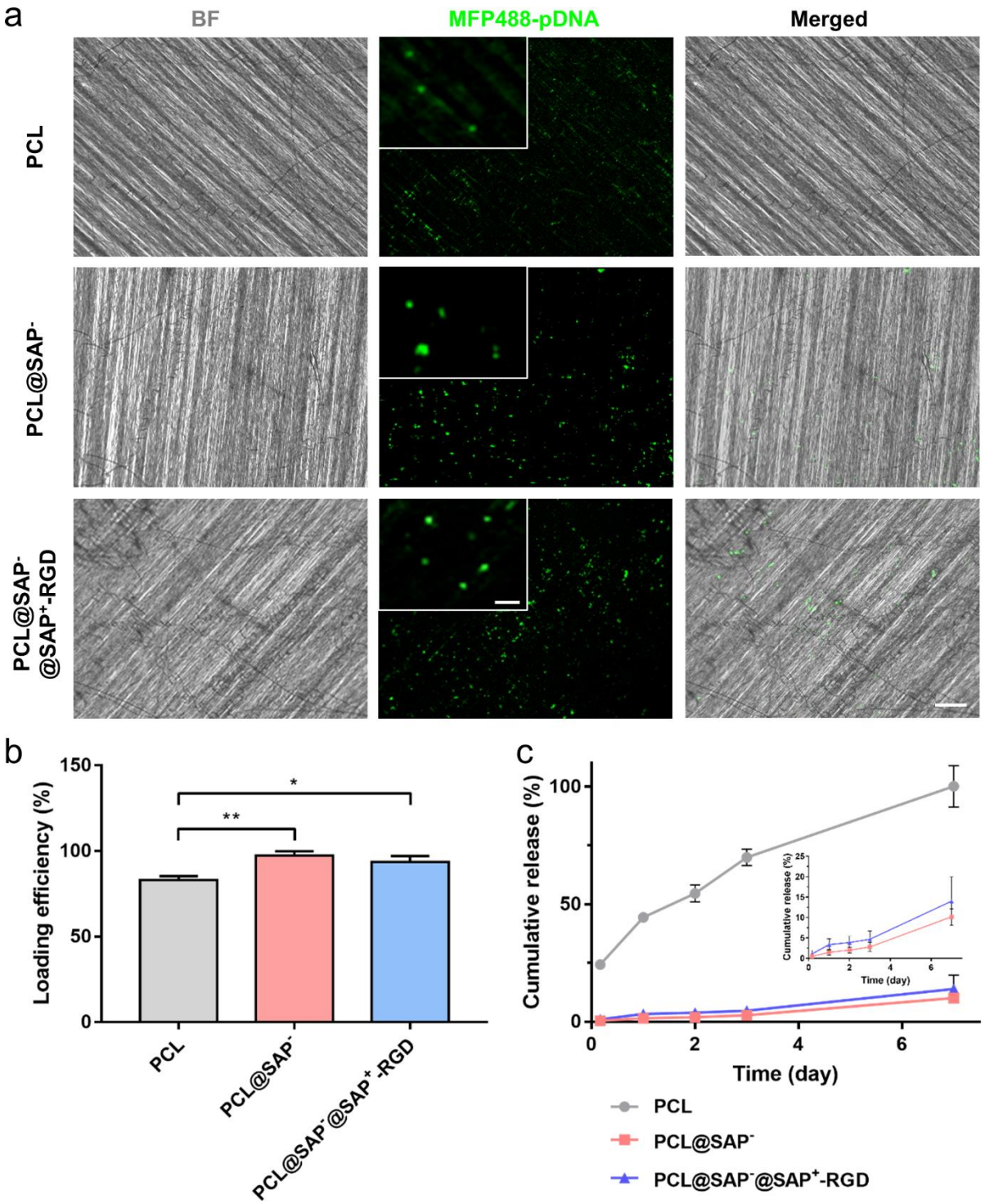


**Fig. 2. Characterization of the loading and release profiles of the pDNA/PEIpro complexes.**

a) Fluorescent images show a uniform distribution of MFP488- pDNA/PEIpro complexes on

aligned fiber substrates. Scale bar = 100 μm (Insert: 10 μm). b) Loading efficiency of pDNA/PEIpro complexes on the scaffolds (n = 3). c) Cumulative release profile of pDNA/PEIpro complexes from scaffolds over 7 days (n = 5).

### *3.3. SAP-coated scaffolds promoted cell adhesion and proliferation*

To better visualize the nanofibers and cell-substrate interactions, Rhodamine B was linked to the N-terminus of $SAP^{-}$. We subsequently examined the effect of SAP coating on cell adhesion by seeding U2OS cells on the scaffolds. As shown in Fig. 3a, after 48 h of culture, only a limited number of cells were observed on the plain PCL scaffolds, while significantly more cells were observed on the PCL@$SAP^{-}$ and PCL@$SAP^{-}$@$SAP^{+}$-RGD scaffolds (Fig. 3b), indicating the improved cell affinity. Similarly, when the cells were cultured in the serum-free medium, the RGD-bearing scaffolds still demonstrated the best cell adhesion performance (Fig. 3c), suggesting that the cells bound directly to RGD instead of the serum proteins that were present in the culture medium. Other than U2OS, these SAP-coated scaffolds can also support the adhesion and spreading of numerous cells, such as human mesenchymal stem cells (hMSCs) and human neural progenitor cells (hNPCs) (Fig. S10). Besides, enhanced cell proliferation was also observed on the PCL@$SAP^{-}$@$SAP^{+}$-RGD scaffolds (Fig. S11). When these SAP-coated scaffolds were subcutaneously implanted, they showed better biocompatibility and cell infiltration *in vivo* (Fig. S12).

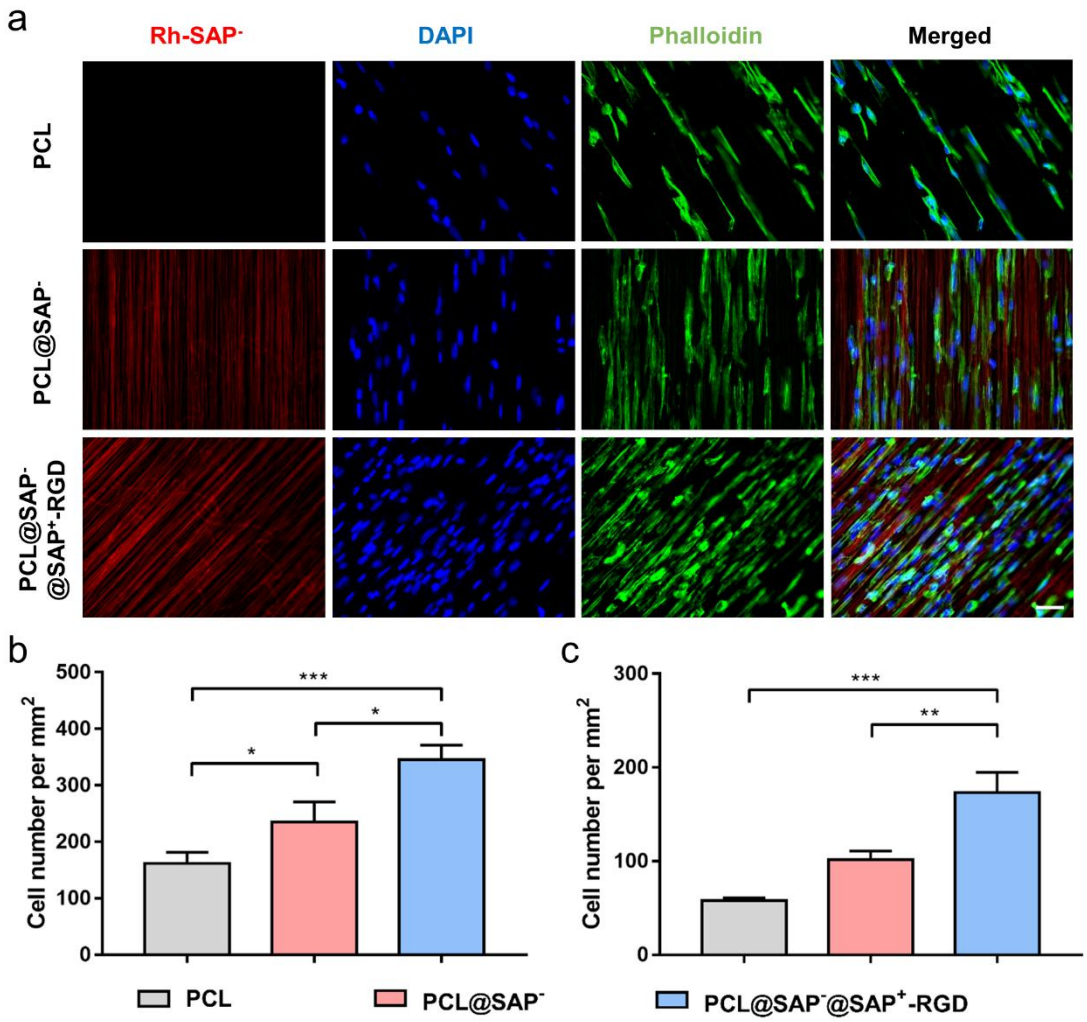


**Fig. 3. SAP coating enhanced cell adhesion on the scaffolds.** a) Representative fluorescent images of U2OS cells on different scaffolds; scale bar = 50 μm. Average cell number per $mm^2$ of U2OS cells after 48 h of culture on scaffolds in b) full medium and c) FBS-free medium for 2 days, respectively (n = 3); $^{*}p < 0.05$, $^{**}p < 0.01$, $^{***}p < 0.001$.

### *3.4. SAP-coated scaffolds facilitated efficient localized gene transfection*

To facilitate the characterization of positive transfection using the CRISPR system, the reporter gene, GFP, was fused to the Cas9 expression cassette [21], and the Cas9-GFP plasmids were used for transfection. As shown in Fig. 4a, the PCL@SAP$^-$@SAP$^+$-RGD group demonstrated the greatest number of GFP-positive cells and the highest intensity of green fluorescence. In comparison, the PCL@SAP$^-$ group showed a smaller number of GFP-positive cells, and the green fluorescence was seldom observed in the absence of SAP coating ("PCL"). The quantitative results confirmed that PCL@SAP$^-$@SAP$^+$-RGD yielded 54.6 GFP$^+$ cells per mm$^2$, whereas PCL@SAP$^-$ and plain PCL only led to 14.4 and 0.7 GFP$^+$ cells per mm$^2$, respectively (Fig. 4b). Meanwhile, although the total cell number on the PCL@SAP$^-$@SAP$^+$-RGD scaffold was significantly higher than the others owing to the enhanced adhesion, this group still showed the best GFP$^+$ percentage (16.1%) among the three groups (Fig. 4c), which is similar to the efficiency of the bolus transfection (18.2%). Furthermore, the gene delivery efficiency was dose-dependent (Fig. S13). Specifically, we found that 4 μg was the optimal amount of plasmid as we started to see toxicity and lower efficiency at 6 μg. We also attempted to assess the transfection efficiency of hNPCs, which are more difficult to be transfected, by seeding these cells on the scaffolds. Correspondingly, we were only able to achieve a much lower transfection efficiency of 9.3% by scaffold-mediated delivery and 11.3% by bolus delivery (Fig. S14).

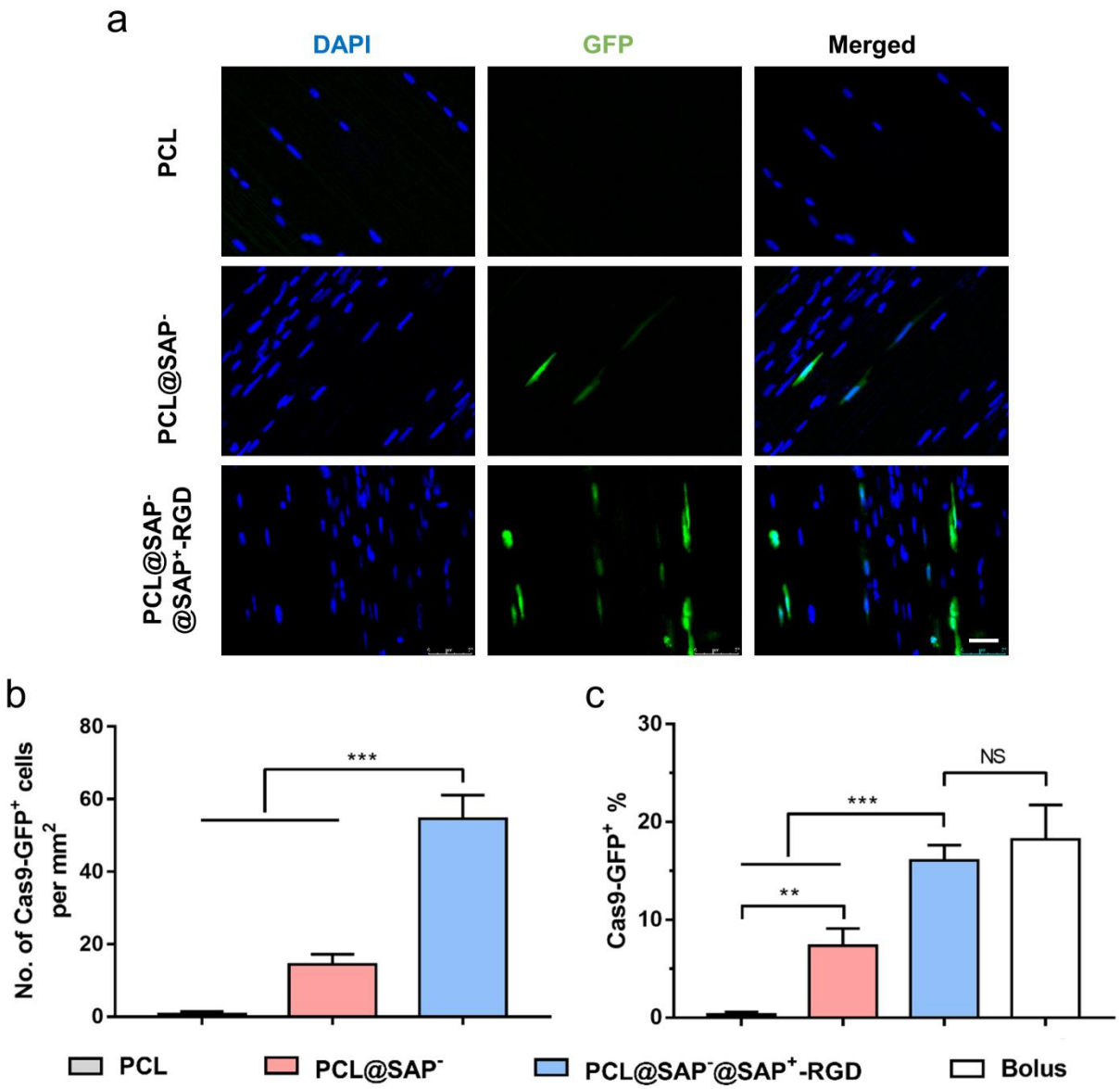


**Fig. 4. SAP-coated scaffolds enhanced the efficiency of Cas9-GFP transfection in mammalian cells.** a) Representative fluorescent images of U2OS cells on different scaffolds; scale bar = 50 μm. Quantification of b) average number of Cas9-GFP$^+$ cells per mm$^2$ and c) transfection efficiency based on fluorescent images (n = 3); $^{**}p < 0.01$, $^{***}p < 0.001$, "NS" indicates "no significance".

### *3.5. Scaffold-mediated CRISPRa system promoted endogenous gene-activation in mammalian cells*

Having established the ability of the SAP-coated scaffolds to facilitate localized gene transfection of mammalian cells, we next examined their specific performance in the delivery of the CRISPRa system and constructed a CRISPRa system targeting hGDNF gene (Fig. 5a). Here, we aimed to utilize GDNF as a proof of concept because the protein secreted is easily detected and quantified, making it a straightforward evaluation of CRISPRa system delivery. The sequences of sgRNAs reported in the literature were ligated into sgRNA expressing vectors and confirmed by DNA sequencing (Table S1, Fig. S15) [26]. We first evaluated the sgRNAs in U2OS cells via co-delivery of sgRNA and dCas9-VPR (i.e., dCas9 fused with a potent tripartite activator, VP64, p65AD and Rta [22]) expressing vectors by bolus transfection, and the treatment significantly increased the mRNA expression of GDNF (Fig. 5b). Meanwhile, it has been reported that multiple sgRNA-dCas9-VP64 complexes can bind to a single promoter, thereby acting synergistically and more efficiently [27]. This synergistic effect was also observed in our experiments and hence the cocktail of sgRNAs (sg01 + 02 + 03) was used in the experiments hereafter.

Subsequently, these pDNA/PEIpro complexes of both sgRNAs and dCas9-VPR expressing vectors were loaded onto the SAP-coated scaffolds, and the U2OS cells were seeded and cultured on the scaffolds. Compared to the non-treated control group, scaffold-mediated transfection of CRISPRa-GDNF resulted in substantial upregulation of GDNF mRNA expression (Fig. 5c). In order to quantify the secretion of GDNF, ELISA was used for the assay of cell culture medium at preset time points. Although the concentration of GDNF in the medium did not change significantly after 24 h, the cells started to produce robust levels of GDNF after 48 h

(Fig. 5d), and the cumulative amount of GDNF secreted in the CRISPRa-GDNF group was also higher than that in the control group (Fig. 5e). However, due to the fast proliferation rate, the cells covered near 90% area of the scaffolds after 72 h, and hence the monitoring of GDNF expression had to be terminated. These results indicated that the CRISPRa system could be loaded onto the scaffolds and delivered to recipient cells for gene engineering.

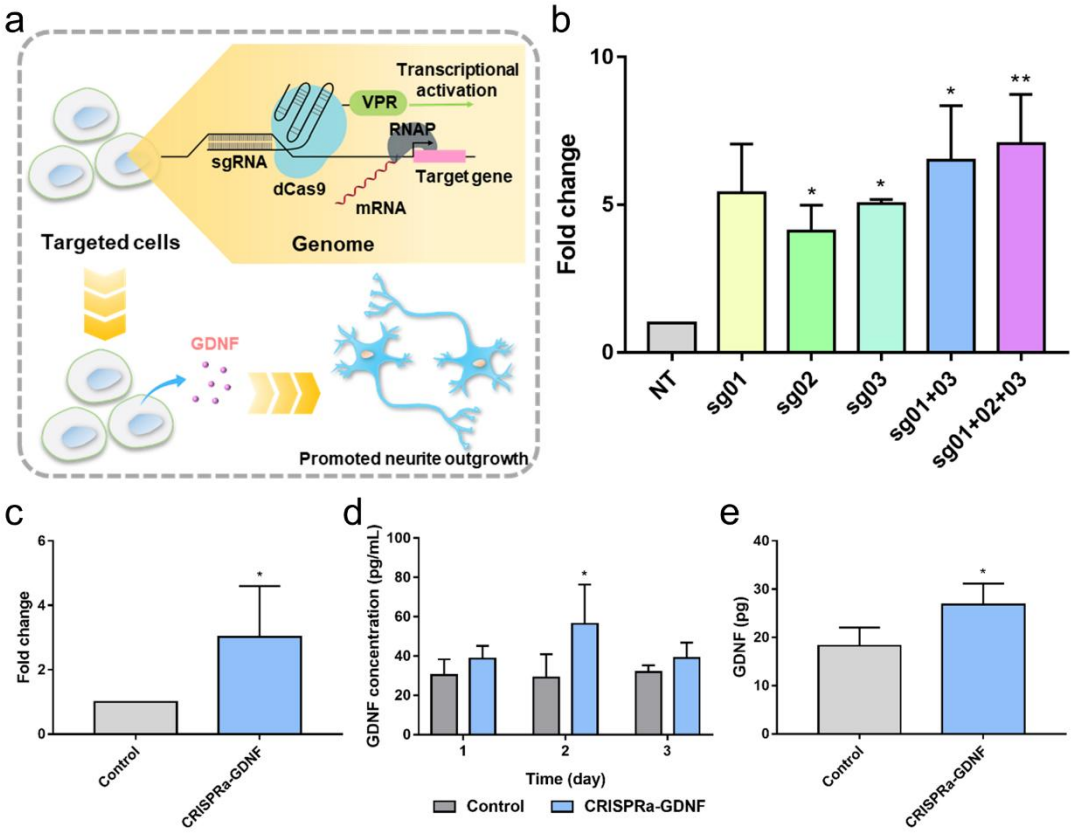


**Fig. 5. SAP-coated scaffolds mediated the delivery of CRISPR/dCas9 based gene activation (CRISPRa-GDNF) system to enhance GDNF mRNA and protein expressions.** a) Schematic representation of the CRISPRa-GDNF system. b) Relative expression of GDNF mRNA in U2OS cells in which the individual or combinations of sgRNAs were co-delivered with dCas9-VPR (n = 3). c) Relative expression of GDNF mRNA, d) GDNF concentration in culture medium at

different time points and e) cumulative GDNF protein expression over 3 days in U2OS cells seeded onto the PCL@SAP$^{-}$@SAP$^{+}$-RGD scaffolds (n = 3); $^{*}p < 0.05$, $^{**}p < 0.01$.

### *3.6. Scaffold-mediated CRISPRa-GDNF system promoted neurite outgrowth*

To further investigate the functional effect of the scaffold-mediated CRISPRa-GDNF system, the ideal experiment would have been a co-culture experiment of U2OS cells and neurons. However, the complexity of keeping both cells alive in the same medium was difficult. The U2OS cells had a high proliferative rate on the scaffolds and would compete for nutrients with the neurons, without adding more media and supplements that might mask the effect of the secreted GDNF. Therefore, we collected the media containing GDNF that were secreted by the U2OS cells seeded on the CRISPRa-functionalized scaffold after 3 days (i.e. conditioned medium), and tested for the bioactivity of the secreted GDNF using primary neurons. Specifically, we transferred the conditioned medium to rat cortical neurons and dorsal root ganglia (DRGs) explants that were cultured on the nanofiber scaffolds for another 3 days. Fig. 6a and b show the representative fluorescent images of cortical neurons and DRGs cultured in culture medium from control and CRISPRa-GDNF scaffolds, respectively, and the neurite outgrowth along the long axis of fibers could be observed. Quantitative analysis confirmed that the CRISPRa-GDNF conditioned medium significantly enhanced neurite outgrowth in both cortical neurons and DRG explants (Fig. 6c and d).

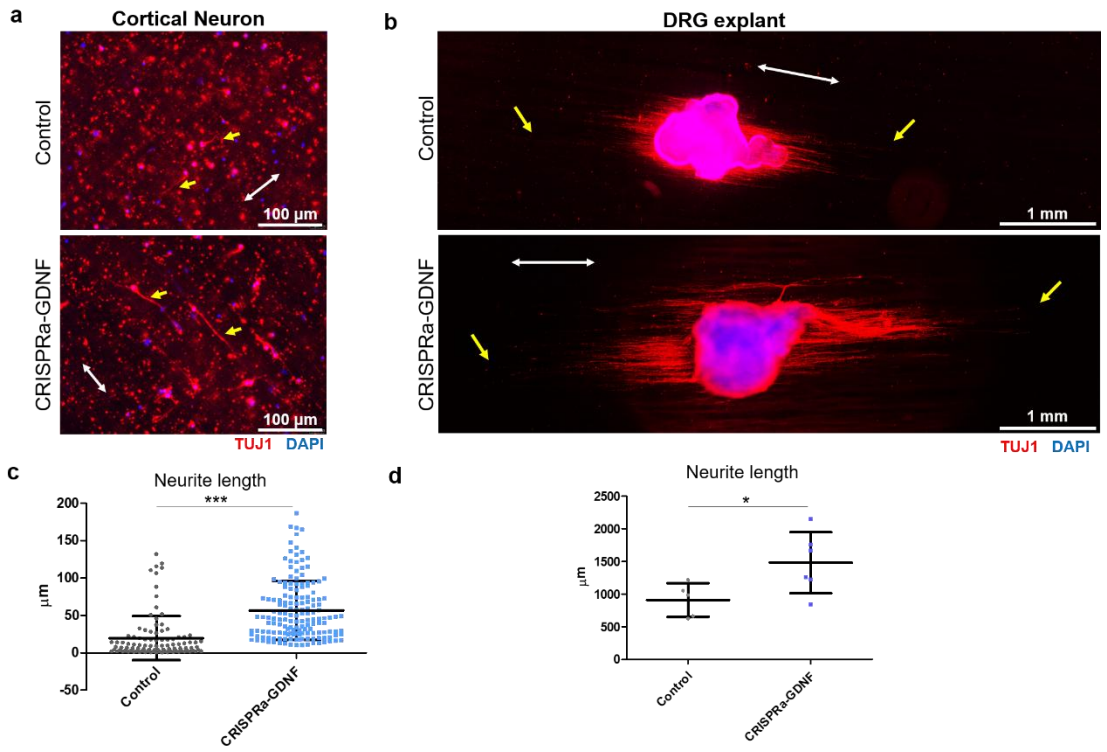


**Fig. 6. Scaffold-mediated CRISPRa-GDNF system promoted neurite outgrowth.** Representative fluorescent images of a) rat cortical neurons and b) DRG explants cultured in control culture medium and CRISPRa-GDNF conditioned medium, respectively. White arrows represent fiber directions while yellow arrows indicate neurites. Quantification of the c) neurite length for cortical neurons (at least 100 neurites from 5 scaffolds each group) and d) average length of 10 longest neurites for DRG explants (n = 5 for control, n = 6 for CRISPRa-GDNF); $^{*}p < 0.05$, $^{**}p < 0.01$.

## 4. Discussion

Biodegradable polymers, such as PCL, are widely used for the fabrication of tissue engineering scaffolds. The chemical and biological stability of PCL makes it difficult for surface

modification. Therefore, simple noncovalent binding are methods usually accompanied by a quick loss of the coating layers due to insufficient interfacial interactions. On the other hand, the chemical modifications typically involve complex, laborious, and environmentally unfriendly chemical synthesis. Utilizing the hydrophobicity of PCL, the SAP coating can alter the surface charge of PCL fiber scaffolds. This approach offers a high level of customization as different peptides can be designed and incorporated into the coating according to specific needs (eg: surfaces with a positive charge, negative charge, cell adhesive peptides, etc). These functionalized SAPs can be coated onto the fibers alone or as a cocktail, and the ratio of different peptides can be adjusted easily. Therefore, the SAP coating is easy-to-implement and sufficiently stable to perform more than one role (eg: immobilization of biomolecules on the surface and support specific cell adhesion).

By altering the surface charge, the PCL@$SAP^-$ group demonstrated improved cell adhesion as compared to plain PCL (Fig. 3), similar to the effect of gas-plasma treatment on cell culture dishes, which makes them more hydrophilic and negatively-charged [28]. We conjugated RGD to the $SAP^+$ as the RGD peptide can be recognized by the integrin subsets and as such may further enhance cell adhesion and spreading (Fig. 3) [29]. Moreover, the SAP backbone can also be conjugated with other peptide sequences other than RGD, such as laminin-derived peptides (IKVAV, YIGSR), N-cadherin mimetic peptide (HAVDI), and Wnt mimetic ligand (MDGECL), thereby offering superb flexibility for various applications [30]. For example, the laminin-derived peptides can be conjugated to enhance neuronal adhesion and neurite outgrowth for neural tissue engineering. Therefore, we herein demonstrate a convenient method for the surface modification of PCL fibers and a promising platform for the investigation of cell-substrate interactions.

In this study, the scaffolds were capable of delivering the CRISPR/dCas9 system in a non-viral manner, which is safer as compared to virus-mediated delivery that raises biosafety concerns. While non-viral polyplexes usually cause some cytotoxicity issues, an optimized delivery method can keep the toxicity under an acceptable level. Here, the cells grew with a high proliferation rate and covered over 90% scaffold area within 3 days, suggesting that the cell viability was acceptable. Such fiber scaffolds also provide more localized and sustained delivery of the CRISPR/dCas9 system than existing methods. In particular, the scaffold-mediated delivery approach ensures localized availability of drugs, which may reduce systemic side effects that is often prominent in systemic delivery approaches. Previous *in vivo* studies showed that similar approaches with scaffold-mediated gene delivery platforms locally released the complexes into the tissues within 300 μm from the edge of the scaffolds [31, 32]. Published results showed that the complexes immobilized on the scaffolds were directly uptaken by the cells from the scaffold surface [14, 18]. Here, Cas9-GFP signals in cells were observed within two days, where the cumulative release was only less than 5%, suggesting that the cells also took up the complexes directly from the scaffold surface. Although there were some larger polyplex aggregates on the scaffold, cellular uptake was not affected as around 97.3 ± 2.4 % cells were found to contain the labelled polyplexes within the cell body (Fig. S16). Furthermore, the modified nanofiber scaffolds can also provide topographical cues for tissue regeneration. In addition to CRISPR/dCas9 system, the coating is expected to be able to immobilize other biomolecules such as nucleic acids (siRNA, miRNA, plasmids) and proteins on the scaffold surfaces.

In addition to the adsorption of CRISPR complexes on the SAP coated nanofibers, the enhanced cellular uptake of the complexes can also be attributed to the increased rate of cell proliferation. The transfection efficiency of the complexes might be affected by the rate of cell

proliferation during which the cell membranes undergo disruption and reconstruction [33]. Here, the U2OS cells proliferated most quickly on the PCL@SAP$^{-}$@SAP$^{+}$-RGD scaffold (Fig. S8), thereby possibly leading to the enhanced uptake of pDNA/PEIpro complexes. However, we did not achieve desirable transfection efficiency with hNPCs, a more realistic model, even by bolus delivery (Fig. S14). One major limitation of this platform is that the transfection efficiency may be affected by the effectiveness and efficiency of the delivery vehicles. Currently, low transfection efficiency is a common problem when transfecting the difficult-to-transfect primary cells, such as hNPCs, hMSCs and dermal fibroblasts [34, 35]. Although PEIpro was shortlisted as the most efficient commercially available transfection reagent through our initial optimization studies (Fig. S14), substituting PEIpro with a better-designed delivery vehicle may further improve the gene delivery efficiency of the scaffold to the hNPCs and neural cells in general. In addition, ribonucleoprotein may be a better format than pDNA in terms of CRISPR complex delivery due to less off-target effects and higher efficiency. As delivery of CRISPR complexes to primary neural cells, particularly post-mitotic neurons, may be challenging, a combination of the improved format (such as ribonucleoprotein) and delivery vehicle will be needed to achieve better results. Furthermore, a comprehensive *in vivo* evaluation of both transfection and gene activation for tissue regeneration will be needed for future pre-clinical studies.

In this study, we only targeted a single gene (GDNF) as a proof of concept. By delivering CRISPRa systems through SAP-coated nanofibers, GDNF expression was activated and hence leading to the production of bioactive GDNF by cells, as demonstrated by the neurite outgrowth assays. While the main objective of this study is to evaluate the ability of the coating to deliver CRISPRa systems, the level of secreted GDNF ($1.0\times10^{-3}$ pg/cell/24h) is comparable to the approaches that directly deliver GDNF transgene ($4.8\times10^{-4}$ to $1.7\times10^{-1}$ pg/cell/24h) and was

effective in stimulating neurite outgrowth [36-40]. GDNF has already been well-established to enhance neurite outgrowth of rat DRG explants and cortical neurons. Hence, we did not include the GDNF-containing media as a positive control to save resources. In the literature, GDNF added at a concentration range of 1 to 100 ng/ml induced 1.5 to 7-folds increase in neurite length of the rat DRG in a dose-dependent manner [41-44]. Similarly, neurite length of rat cortical neurons increased 1.2 to 3-folds in the presence of 0.1 to 100 ng/ml GDNF in a dose-dependent manner [45-47]. The increase in neurite length of DRG and cortical neurons in our experiment were about 1.5-folds and 2-folds of the control respectively, which are within the range of the published results. A small amount of GDNF as little as 70 pg/ml could stimulate neurite outgrowth of spinal neurons [48].

In addition, the CRISPRa system is also capable of targeting multiple genes, requiring only additional sgRNAs. Future works may extend the application of the CRISPRa systems-loaded platform to relevant primary cells, such as glia and meningeal cells, which could be ideal targets *in vivo* to secrete GDNF locally to enhance nerve regeneration. This ability of selective gene upregulation provides a promising strategy to direct stem or progenitor cell differentiation for regenerative medicine applications [49]. For example, these scaffolds are expected to be capable of localized delivery of CRISPR/dCas9 to direct neuronal differentiation of stem cells through the activation of transcription factors, which will contribute to neural regeneration as well [50, 51]. Besides the CRISPRa system, this scaffold-mediated CRISPR delivery system is also suitable for CRISPR knockout (CRISPRko) and CRISPRi systems when the corresponding sgRNAs and Cas9 or dCas9 expressing vectors are utilized.

## 5. Conclusion

In summary, we synthesized two amphiphilic SAPs with opposite net charges, $SAP^-$ and $SAP^+$-RGD. The SAP was first coated onto PCL nanofibers through strong hydrophobic interactions, and the pDNA/PEIpro complexes and $SAP^+$-RGD were then easily absorbed via electrostatic interactions. The SAP-coated scaffolds facilitated efficient loading and sustained release of the pDNA complexes, while similar amount of pDNA complexes were completely released from plain PCL scaffolds within 7 days. Meanwhile, the SAP coating effectively enhanced cell adhesion and proliferation, even in the absence of serum proteins ($p < 0.0001$). Therefore, these scaffolds were utilized for the localized delivery of the CRISPR/dCas9 system, which activated GDNF expression in mammalian cells and produced GDNF ($1.0\times10^{-3}$ pg/cell/24h). The secreted GDNF retained its bioactivity and promoted neurite outgrowth, as evidenced by the twice longer neurites than the non-treated groups. All these promising results indicate that LbL SAP-coated nanofibers provide a useful tool for non-viral genome editing. Together with the continuously developing CRISPR techniques, such scaffolds demonstrate great potential in tissue regeneration.

## Competing interest

The authors declare no conflict of interest.

## Acknowledgment

This research is supported by the A*Star BMRC International Joint Grant – Singapore-China Joint Research Program (Project no. 1610500024) and MOE AcRF Tier 1 Grant (Project No:

RG148/14) awarded to SYC. The authors would like to thank Prof Hai-quan Mao (Johns Hopkins University), Prof Kam Leong and Dr Hongxia Wang (Columbia University), Dr Chuntao Liu (Sun Yat-sen University), Na Zhang, Junquan Lin, and William Ong (Nanyang Technological University) for insightful suggestion and discussion, and Prof Sierin Lim (Nanyang Technological University) for providing the E. Coli culture facilities.

## References

[1] P.D. Hsu, E.S. Lander, F. Zhang, Development and applications of CRISPR-Cas9 for genome engineering, Cell 157(6) (2014) 1262-78.
[2] D.B. Cox, R.J. Platt, F. Zhang, Therapeutic genome editing: prospects and challenges, Nat Med 21(2) (2015) 121-31.
[3] P. Perez-Pinera, D.D. Kocak, C.M. Vockley, A.F. Adler, A.M. Kabadi, L.R. Polstein, P.I. Thakore, K.A. Glass, D.G. Ousterout, K.W. Leong, F. Guilak, G.E. Crawford, T.E. Reddy, C.A. Gersbach, RNA-guided gene activation by CRISPR-Cas9-based transcription factors, Nat Methods 10(10) (2013) 973-6.
[4] M.H. Hanewich-Hollatz, Z. Chen, L.M. Hochrein, J. Huang, N.A. Pierce, Conditional guide RNAs: programmable conditional regulation of CRISPR/Cas function in bacterial and mammalian cells via dynamic RNA nanotechnology, ACS central science 5(7) (2019) 1241-1249.
[5] M.F. La Russa, L.S. Qi, The New State of the Art: Cas9 for Gene Activation and Repression, Mol Cell Biol 35(22) (2015) 3800-9.
[6] M.H. Larson, L.A. Gilbert, X. Wang, W.A. Lim, J.S. Weissman, L.S. Qi, CRISPR interference (CRISPRi) for sequence-specific control of gene expression, Nature protocols 8(11) (2013) 2180.
[7] P. Perez-Pinera, D.D. Kocak, C.M. Vockley, A.F. Adler, A.M. Kabadi, L.R. Polstein, P.I. Thakore, K.A. Glass, D.G. Ousterout, K.W. Leong, RNA-guided gene activation by CRISPR-Cas9–based transcription factors, Nature methods 10(10) (2013) 973.
[8] S.M. Czerniecki, N.M. Cruz, J.L. Harder, R. Menon, J. Annis, E.A. Otto, R.E. Gulieva, L.V. Islas, Y.K. Kim, L.M. Tran, T.J. Martins, J.W. Pippin, H. Fu, M. Kretzler, S.J. Shankland, J. Himmelfarb, R.T. Moon, N. Paragas, B.S. Freedman, High-Throughput Screening Enhances Kidney Organoid Differentiation from Human Pluripotent Stem Cells and Enables Automated Multidimensional Phenotyping, Cell Stem Cell 22(6) (2018) 929-940 e4.
[9] H.X. Wang, M. Li, C.M. Lee, S. Chakraborty, H.W. Kim, G. Bao, K.W. Leong, CRISPR/Cas9-Based Genome Editing for Disease Modeling and Therapy: Challenges and Opportunities for Nonviral Delivery, Chem Rev 117(15) (2017) 9874-9906.
[10] D.G. Tamay, T. Dursun Usal, A.S. Alagoz, D. Yucel, N. Hasirci, V. Hasirci, 3D and 4D Printing of Polymers for Tissue Engineering Applications, Front Bioeng Biotechnol 7 (2019) 164.

[11] A. Cipitria, A. Skelton, T.R. Dargaville, P.D. Dalton, D.W. Hutmacher, Design, fabrication and characterization of PCL electrospun scaffolds—a review, Journal of Materials Chemistry 21(26) (2011) 9419-9453.
[12] H.J. Diao, W.C. Low, U. Milbreta, Q.R. Lu, S.Y. Chew, Nanofiber-mediated microRNA delivery to enhance differentiation and maturation of oligodendroglial precursor cells, J Control Release 208 (2015) 85-92.
[13] W.C. Low, P.O. Rujitanaroj, D.K. Lee, P.B. Messersmith, L.W. Stanton, E. Goh, S.Y. Chew, Nanofibrous scaffold-mediated REST knockdown to enhance neuronal differentiation of stem cells, Biomaterials 34(14) (2013) 3581-90.
[14] W.H. Chooi, W. Ong, A. Murray, J. Lin, D. Nizetic, S.Y. Chew, Scaffold mediated gene knockdown for neuronal differentiation of human neural progenitor cells, Biomater Sci 6(11) (2018) 3019-3029.
[15] J. Lin, D. Anopas, U. Milbreta, P.H. Lin, J.S. Chin, N. Zhang, S.K. Wee, A. Tow, W.T. Ang, S.Y. Chew, Regenerative rehabilitation: exploring the synergistic effects of rehabilitation and implantation of a bio-functional scaffold in enhancing nerve regeneration, Biomater Sci 7(12) (2019) 5150-5160.
[16] W. Ong, J. Lin, M.E. Bechler, K. Wang, M. Wang, C. Ffrench-Constant, S.Y. Chew, Microfiber drug/gene delivery platform for study of myelination, Acta Biomater 75 (2018) 152-160.
[17] H.J. Diao, W.C. Low, Q.R. Lu, S.Y. Chew, Topographical effects on fiber-mediated microRNA delivery to control oligodendroglial precursor cells development, Biomaterials 70 (2015) 105-14.
[18] J.S. Chin, W.H. Chooi, H. Wang, W. Ong, K.W. Leong, S.Y. Chew, Scaffold-mediated non-viral delivery platform for CRISPR/Cas9-based genome editing, Acta Biomater 90 (2019) 60-70.
[19] S. Jo, S.M. Kang, S.A. Park, W.D. Kim, J. Kwak, H. Lee, Enhanced adhesion of preosteoblasts inside 3D PCL scaffolds by polydopamine coating and mineralization, Macromol Biosci 13(10) (2013) 1389-95.
[20] L. Li, S. Hu, X. Chen, Non-viral delivery systems for CRISPR/Cas9-based genome editing: Challenges and opportunities, Biomaterials 171 (2018) 207-218.
[21] F.A. Ran, P.D. Hsu, J. Wright, V. Agarwala, D.A. Scott, F. Zhang, Genome engineering using the CRISPR-Cas9 system, Nat Protoc 8(11) (2013) 2281-2308.
[22] A. Chavez, J. Scheiman, S. Vora, B.W. Pruitt, M. Tuttle, P.R.I. E, S. Lin, S. Kiani, C.D. Guzman, D.J. Wiegand, D. Ter-Ovanesyan, J.L. Braff, N. Davidsohn, B.E. Housden, N. Perrimon, R. Weiss, J. Aach, J.J. Collins, G.M. Church, Highly efficient Cas9-mediated transcriptional programming, Nat Methods 12(4) (2015) 326-8.
[23] A. Murray, A. Letourneau, C. Canzonetta, E. Stathaki, S. Gimelli, F. Sloan-Bena, R. Abrehart, P. Goh, S. Lim, C. Baldo, F. Dagna-Bricarelli, S. Hannan, M. Mortensen, D. Ballard, D. Syndercombe Court, N. Fusaki, M. Hasegawa, T.G. Smart, C. Bishop, S.E. Antonarakis, J. Groet, D. Nizetic, Brief report: isogenic induced pluripotent stem cell lines from an adult with mosaic down syndrome model accelerated neuronal ageing and neurodegeneration, Stem Cells 33(6) (2015) 2077-84.
[24] N. Zhang, U. Milbreta, J.S. Chin, C. Pinese, J. Lin, H. Shirahama, W. Jiang, H. Liu, R. Mi, A. Hoke, W. Wu, S.Y. Chew, Biomimicking Fiber Scaffold as an Effective In Vitro and In Vivo MicroRNA Screening Platform for Directing Tissue Regeneration, Adv Sci (Weinh) 6(9) (2019) 1800808.

[25] L. Delafosse, P. Xu, Y. Durocher, Comparative study of polyethylenimines for transient gene expression in mammalian HEK293 and CHO cells, J Biotechnol 227 (2016) 103-111.
[26] S. Konermann, M.D. Brigham, A.E. Trevino, J. Joung, O.O. Abudayyeh, C. Barcena, P.D. Hsu, N. Habib, J.S. Gootenberg, H. Nishimasu, O. Nureki, F. Zhang, Genome-scale transcriptional activation by an engineered CRISPR-Cas9 complex, Nature 517(7536) (2015) 583-8.
[27] M.L. Maeder, S.J. Linder, V.M. Cascio, Y. Fu, Q.H. Ho, J.K. Joung, CRISPR RNA-guided activation of endogenous human genes, Nat Methods 10(10) (2013) 977-9.
[28] M.J. Lerman, J. Lembong, S. Muramoto, G. Gillen, J.P. Fisher, The Evolution of Polystyrene as a Cell Culture Material, Tissue Eng Part B Rev 24(5) (2018) 359-372.
[29] E. Ruoslahti, RGD and other recognition sequences for integrins, Annu Rev Cell Dev Biol 12 (1996) 697-715.
[30] N. Huettner, T.R. Dargaville, A. Forget, Discovering Cell-Adhesion Peptides in Tissue Engineering: Beyond RGD, Trends Biotechnol 36(4) (2018) 372-383.
[31] L.H. Nguyen, M. Gao, J. Lin, W. Wu, J. Wang, S.Y. Chew, Three-dimensional aligned nanofibers-hydrogel scaffold for controlled non-viral drug/gene delivery to direct axon regeneration in spinal cord injury treatment, Sci Rep 7 (2017) 42212.
[32] C. Pinese, J. Lin, U. Milbreta, M. Li, Y. Wang, K.W. Leong, S.Y. Chew, Sustained delivery of siRNA/mesoporous silica nanoparticle complexes from nanofiber scaffolds for long-term gene silencing, Acta Biomater 76 (2018) 164-177.
[33] S. Chernousova, M. Epple, Live-cell imaging to compare the transfection and gene silencing efficiency of calcium phosphate nanoparticles and a liposomal transfection agent, Gene Ther 24(5) (2017) 282-289.
[34] Y. Wang, L. Wang, Y. Zhu, J. Qin, Human brain organoid-on-a-chip to model prenatal nicotine exposure, Lab Chip 18(6) (2018) 851-860.
[35] O. Gresch, L. Altrogge, Transfection of difficult-to-transfect primary mammalian cells, Methods Mol Biol 801 (2012) 65-74.
[36] A. Sajadi, J.C. Bensadoun, B.L. Schneider, C. Lo Bianco, P. Aebischer, Transient striatal delivery of GDNF via encapsulated cells leads to sustained behavioral improvement in a bilateral model of Parkinson disease, Neurobiol Dis 22(1) (2006) 119-29.
[37] M. Suzuki, J. McHugh, C. Tork, B. Shelley, A. Hayes, I. Bellantuono, P. Aebischer, C.N. Svendsen, Direct muscle delivery of GDNF with human mesenchymal stem cells improves motor neuron survival and function in a rat model of familial ALS, Mol Ther 16(12) (2008) 2002-10.
[38] M. Suzuki, J. McHugh, C. Tork, B. Shelley, S.M. Klein, P. Aebischer, C.N. Svendsen, GDNF secreting human neural progenitor cells protect dying motor neurons, but not their projection to muscle, in a rat model of familial ALS, PLoS One 2(8) (2007) e689.
[39] A.A. Akhtar, G. Gowing, N. Kobritz, S.E. Savinoff, L. Garcia, D. Saxon, N. Cho, G. Kim, C.M. Tom, H. Park, G. Lawless, B.C. Shelley, V.B. Mattis, J.J. Breunig, C.N. Svendsen, Inducible Expression of GDNF in Transplanted iPSC-Derived Neural Progenitor Cells, Stem Cell Reports 10(6) (2018) 1696-1704.
[40] A. Bakshi, S. Shimizu, C.A. Keck, S. Cho, D.G. LeBold, D. Morales, E. Arenas, E.Y. Snyder, D.J. Watson, T.K. McIntosh, Neural progenitor cells engineered to secrete GDNF show enhanced survival, neuronal differentiation and improve cognitive function following traumatic brain injury, Eur J Neurosci 23(8) (2006) 2119-34.

[41] C. Deister, C.E. Schmidt, Optimizing neurotrophic factor combinations for neurite outgrowth, J Neural Eng 3(2) (2006) 172-9.
[42] D. Santos, F. Gonzalez-Perez, X. Navarro, J. Del Valle, Dose-Dependent Differential Effect of Neurotrophic Factors on In Vitro and In Vivo Regeneration of Motor and Sensory Neurons, Neural Plast 2016 (2016) 4969523.
[43] S. Takaku, H. Yanagisawa, K. Watabe, H. Horie, T. Kadoya, K. Sakumi, Y. Nakabeppu, F. Poirier, K. Sango, GDNF promotes neurite outgrowth and upregulates galectin-1 through the RET/PI3K signaling in cultured adult rat dorsal root ganglion neurons, Neurochem Int 62(3) (2013) 330-9.
[44] W.A. Lackington, Z. Koci, T. Alekseeva, A.J. Hibbitts, S.L. Kneafsey, G. Chen, F.J. O'Brien, Controlling the dose-dependent, synergistic and temporal effects of NGF and GDNF by encapsulation in PLGA microparticles for use in nerve guidance conduits for the repair of large peripheral nerve defects, J Control Release 304 (2019) 51-64.
[45] R. Pellitteri, A. Russo, S. Stanzani, D. Zaccheo, Olfactory ensheathing cells protect cortical neuron cultures exposed to hypoxia, CNS Neurol Disord Drug Targets 14(1) (2015) 68-76.
[46] J. Nielsen, K. Gotfryd, S. Li, N. Kulahin, V. Soroka, K.K. Rasmussen, E. Bock, V. Berezin, Role of glial cell line-derived neurotrophic factor (GDNF)-neural cell adhesion molecule (NCAM) interactions in induction of neurite outgrowth and identification of a binding site for NCAM in the heel region of GDNF, J Neurosci 29(36) (2009) 11360-76.
[47] C. Tohda, E. Joyashiki, Sominone enhances neurite outgrowth and spatial memory mediated by the neurotrophic factor receptor, RET, Br J Pharmacol 157(8) (2009) 1427-40.
[48] W. Gu, F. Zhang, Q. Xue, Z. Ma, P. Lu, B. Yu, Bone mesenchymal stromal cells stimulate neurite outgrowth of spinal neurons by secreting neurotrophic factors, Neurol Res 34(2) (2012) 172-80.
[49] Z. Zhang, Y. Zhang, F. Gao, S. Han, K.S. Cheah, H.F. Tse, Q. Lian, CRISPR/Cas9 Genome-Editing System in Human Stem Cells: Current Status and Future Prospects, Mol Ther Nucleic Acids 9 (2017) 230-241.
[50] J. Shao, M. Wang, G. Yu, S. Zhu, Y. Yu, B.C. Heng, J. Wu, H. Ye, Synthetic far-red light-mediated CRISPR-dCas9 device for inducing functional neuronal differentiation, Proc Natl Acad Sci U S A 115(29) (2018) E6722-E6730.
[51] J.B. Black, A.F. Adler, H.G. Wang, A.M. D'Ippolito, H.A. Hutchinson, T.E. Reddy, G.S. Pitt, K.W. Leong, C.A. Gersbach, Targeted Epigenetic Remodeling of Endogenous Loci by CRISPR/Cas9-Based Transcriptional Activators Directly Converts Fibroblasts to Neuronal Cells, Cell Stem Cell 19(3) (2016) 406-14.

## Graphical abstract

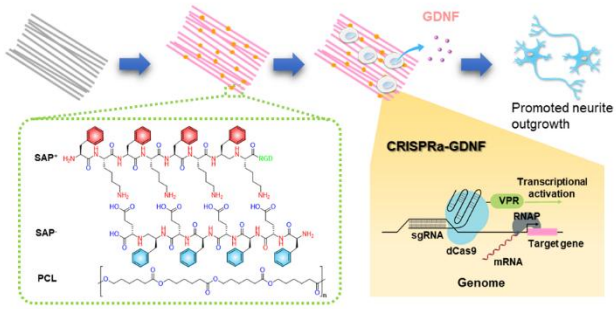

**Supplementary Information**

**Click here to download Supplementary Files: Revised Supplementary Information.DOCX**

**Manuscript with changes tracked**

**Click here to download Supplementary Files: Revised manuscript_changes marked.DOCX**

**Supplementary Information with changes tracked**

**Click here to download Supplementary Files: Revised Supplementary Information_changes marked.DOCX**

***Declaration of Interest Statement**

**Declaration of interests**

☒ The authors declare that they have no known competing financial interests or personal relationships that could have appeared to influence the work reported in this paper.

☐The authors declare the following financial interests/personal relationships which may be considered as potential competing interests: